Electronic Supplementary Material (ESI) for Journal of Materials Chemistry A.

Electronic Supplementary Information

Rational Design of High Nitrogen-Doped and Core-Shell/Mesoporous Carbon Nanospheres with High Rate Capability and Cycling Longevity for Pseudocapacitive Sodium Storage

Jiayi Mao,[a] Dechao Niu,*,[a] Nan Jiang, [a] Guangyu Jiang,[a] Meiwan Chen, [a] Yongsheng Li,*,[a] and Jianlin Shi [a,b]

[a] Lab of Low-Dimensional Materials Chemistry, Key Laboratory for Ultrafine Materials of Ministry of Education, School of Materials Science and Engineering, East China University of Science and Technology, Shanghai 200237, China.

Corresponding Email: dcniu@ecust.edu.cn, ysli@ecust.edu.cn

[b] State Key Laboratory of High-Performance Ceramics and Superfine Microstructure, Shanghai Institute of Ceramics, Chinese Academy of Sciences, Shanghai 200050, China

This file includes:

Fig. S1 − 17

Table S1 – 3

References S1-7

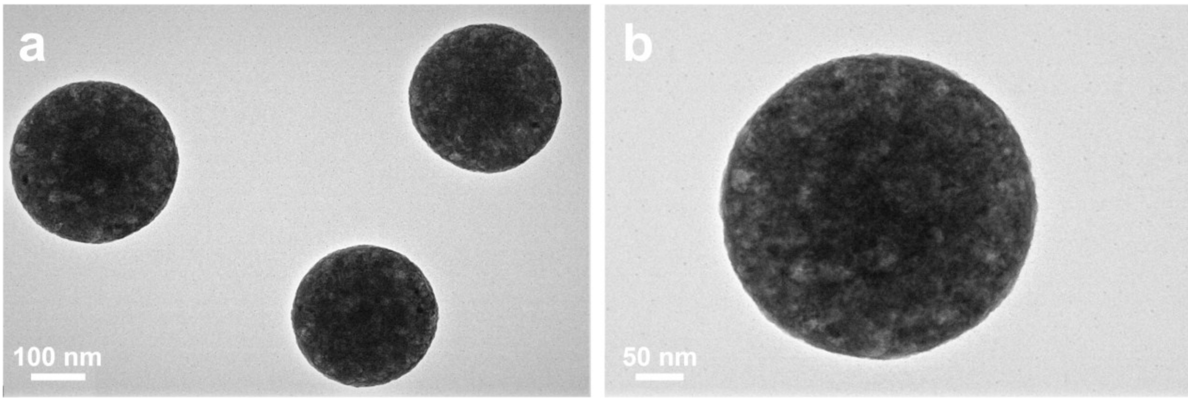

Fig. S1 TEM images of spherical composite micelles at different magnifications.

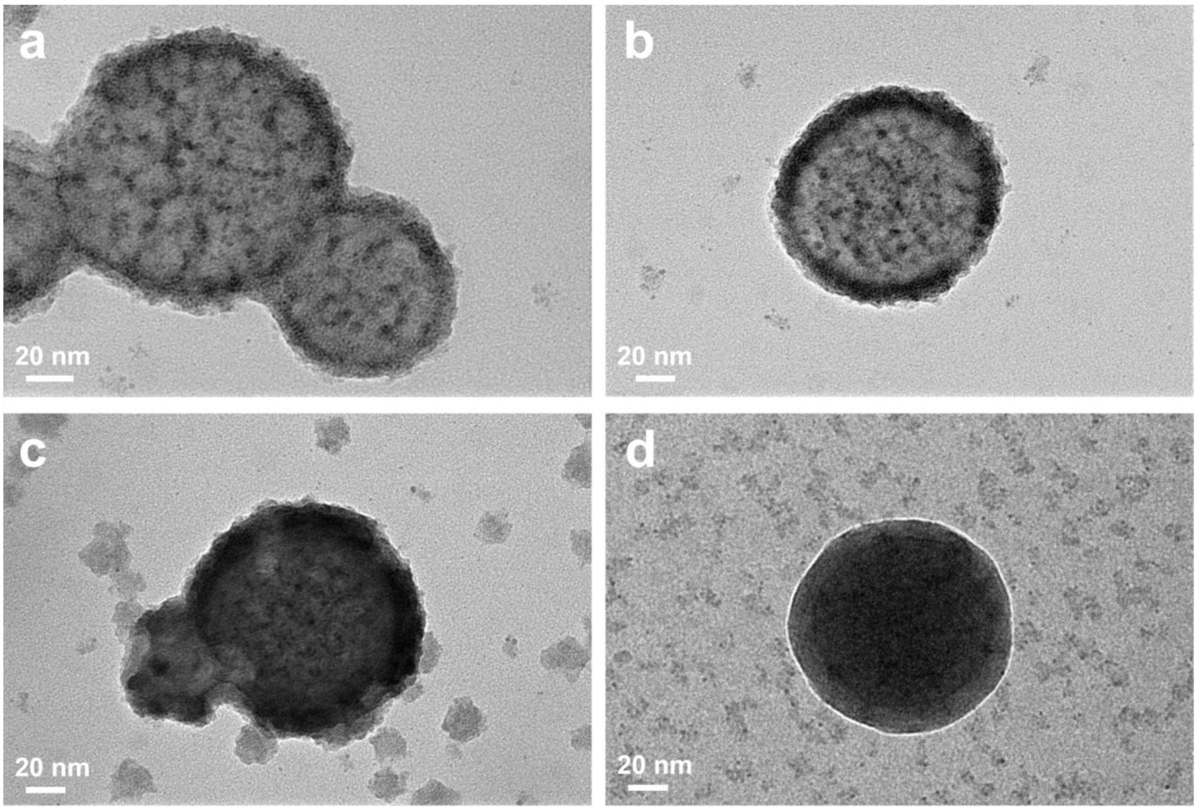

Fig. S2 TEM images of the composite micelles with PDA obtained by different reaction time periods: (a) 1 h, (b) 4 h, (c) 8 h, (d) 20 h.

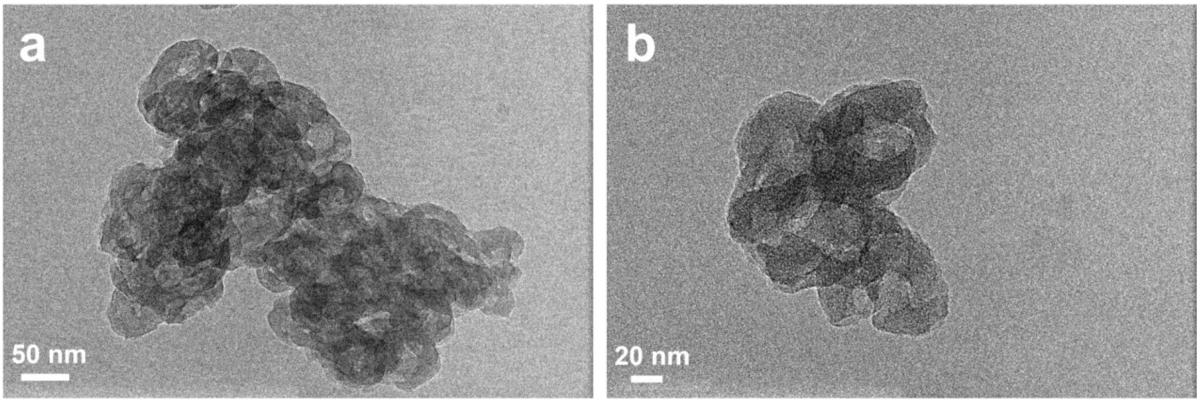

Fig. S3 TEM images of the control group synthesized in almost the same way as HN-CSMCNs without the addition of CATB.

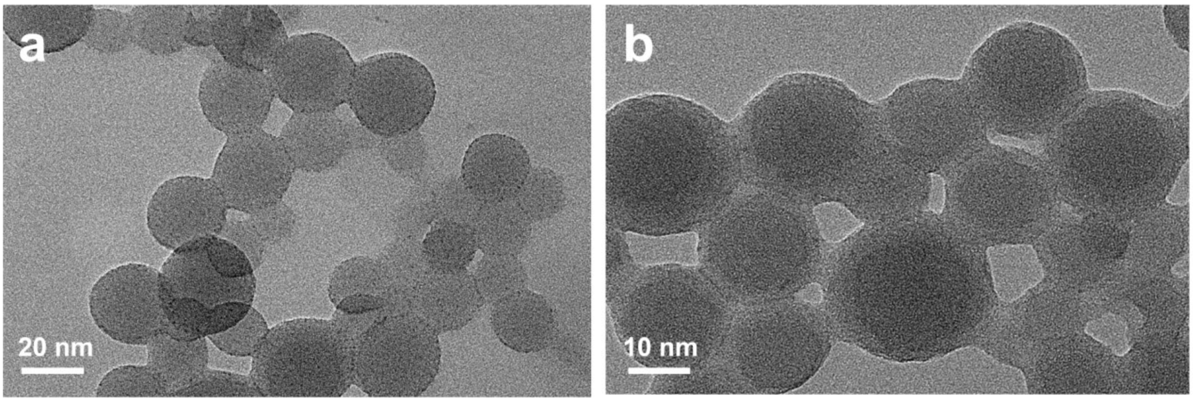

Fig. S4 TEM images of pure PS-*b*-PAA micelles.

Table S1 BET surface areas, pore volumes and pore size distributions of HN-CSMCNs, HN-HCNs and N-CSMCNs.

Samples	Specific surface area (m^2 g^{-1})	Pore volume (cm^3 g^{-1})	Mesopore size (nm)
HN-CSMCNs	449	0.60	14.8
HN-HCNs	310	0.34	/
N-CSMCNs	415	0.53	15.6

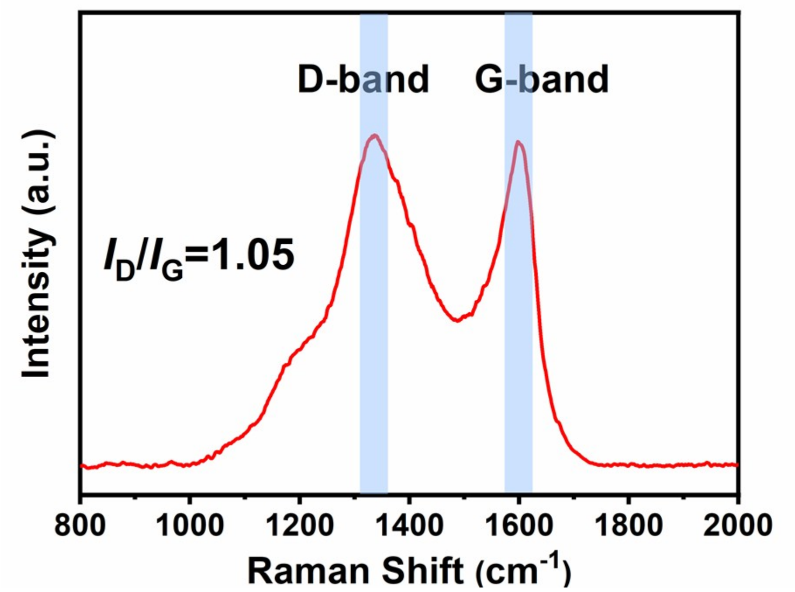

Fig. S5 Raman spectrum of HN-CSMCNs.

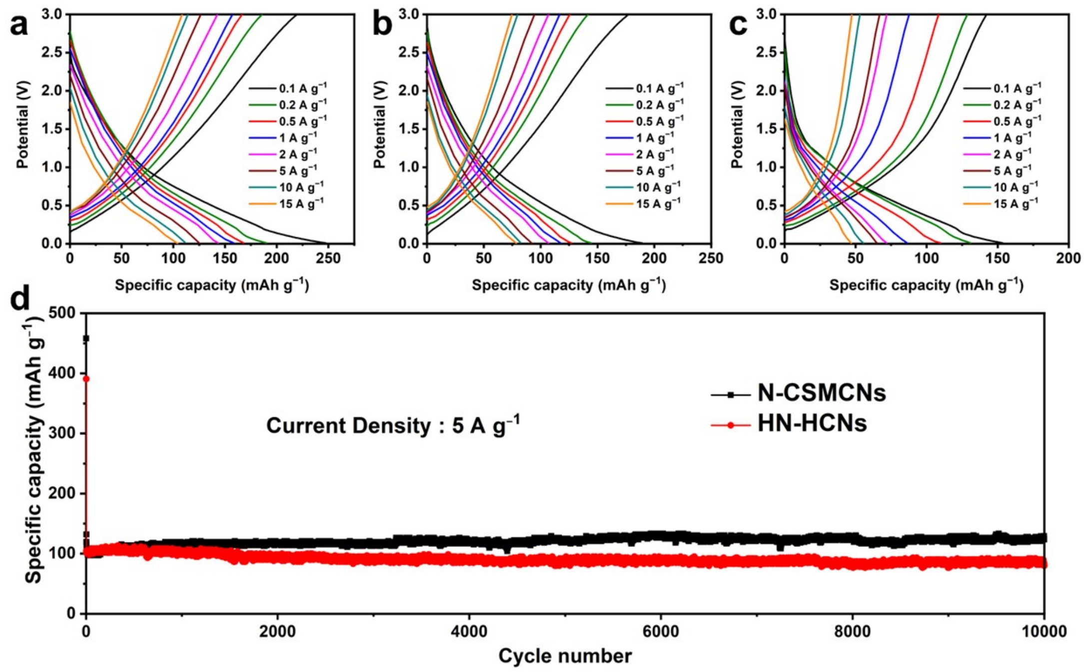

Fig. S6 (a-c) The galvanostatic discharge/charge curves of the HN-CSMCNs, HN-HCNs and N-CSMCNs, (d) the cycling performances of N-CSMCNs and HN-HCNs at 5 A g^{-1}.

Table S2 Comparison of detailed XPS results for HN-CSMCNs, HN-HCNs and N-CSMCNs.

Sample	Carbon (wt%)	Nitrogen (wt%)	Oxygen (wt%)	Pyridinic N (%)	Pyrrolic N (%)	Graphitic N (%)	Oxidized N (%)
HN-CSMCNs	85.45	10.07	4.48	32.80	25.48	32.80	8.92
HN-HCNs	85.63	9.65	4.73	30.77	24.24	35.53	9.47
N-CSMCNs	88.57	6.43	5.00	22.26	16.96	49.35	11.43

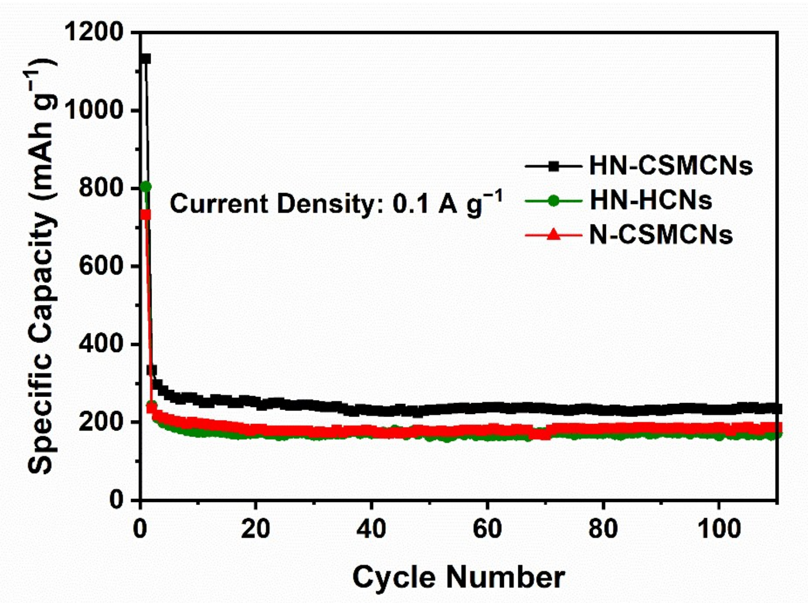

Fig. S7 Cycling performances of HN-CSMCNs, HN-HCNs and N-CSMCNs at 0.1 A g^{-1}.

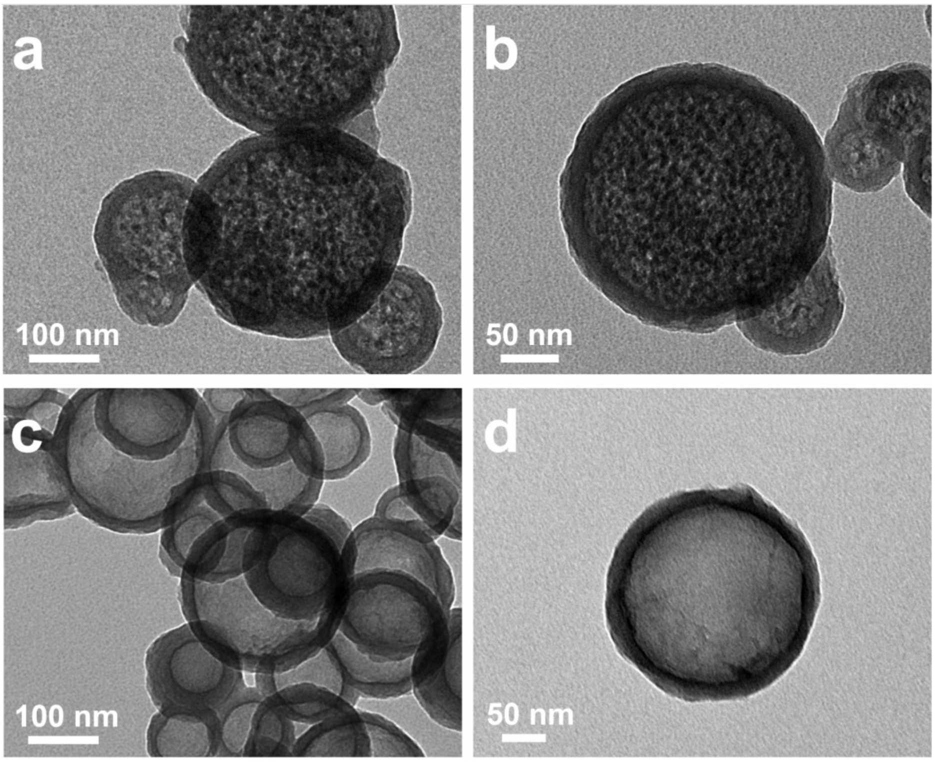

Fig. S8 TEM images of (a, b) N-CSMCNs and (c, d) HN-HCNs.

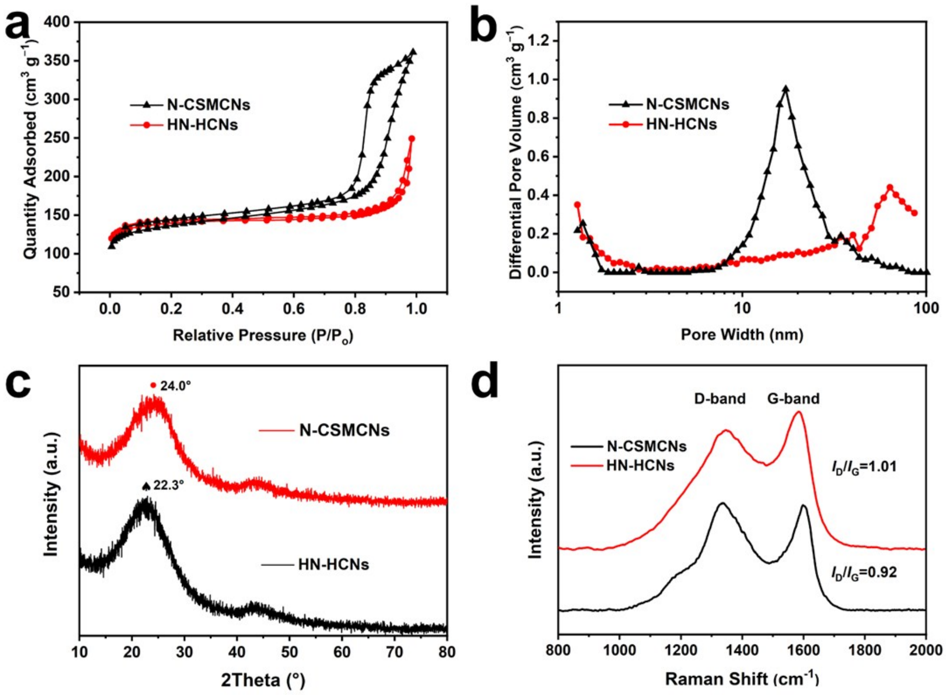

Fig. S9 (a) Nitrogen adsorption/desorption isotherms, (b) BJH pore size distributions from absorption branches, (c) XRD patterns and (d) Raman spectra of N-CSMCNs and HN-HCNs.

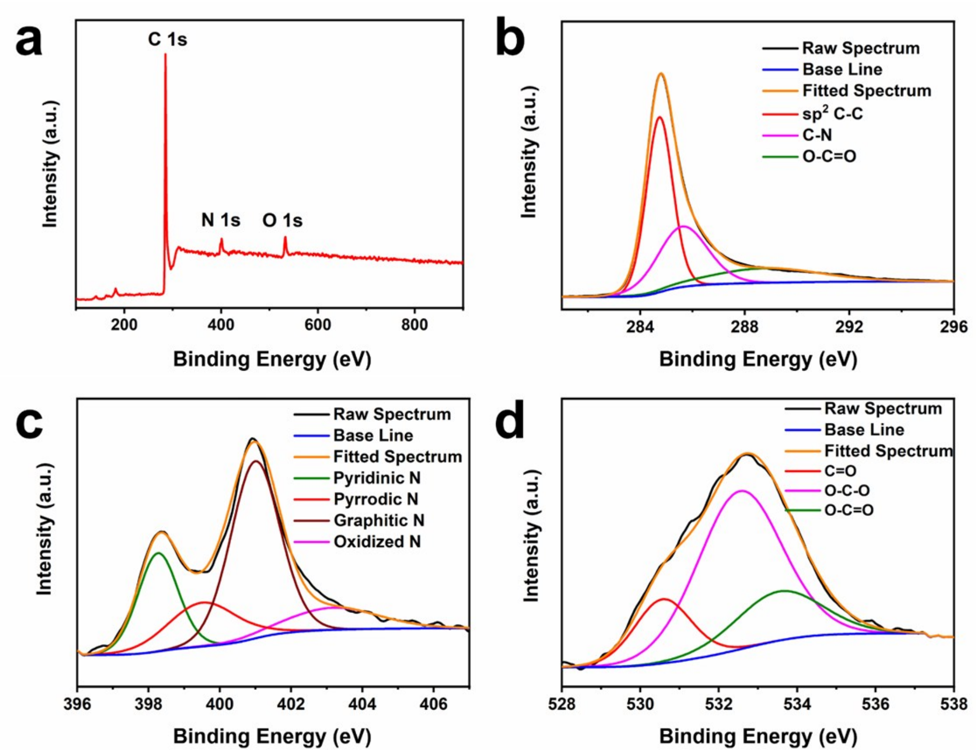

Fig S10. (a) XPS survey spectrum, (b) C 1s, (c) N 1s, and (d) C 1s spectra of N-CSMCNs.

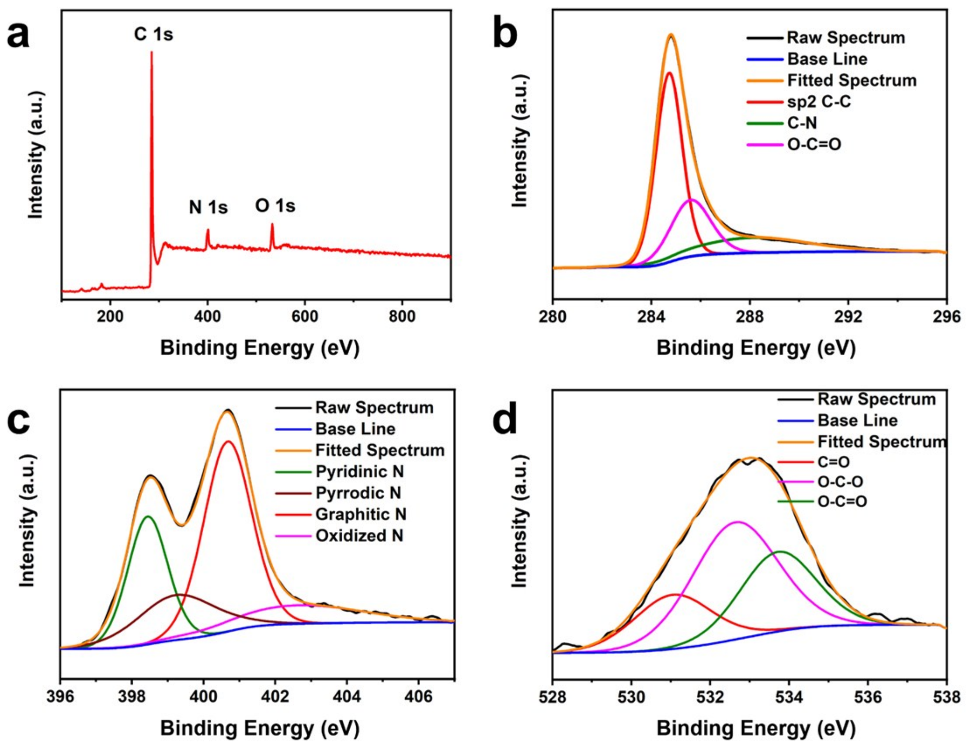

Fig. S11 (a) XPS survey spectrum, (b) C 1s, (c) N 1s, and (d) C 1s spectra of HN-HCNs.

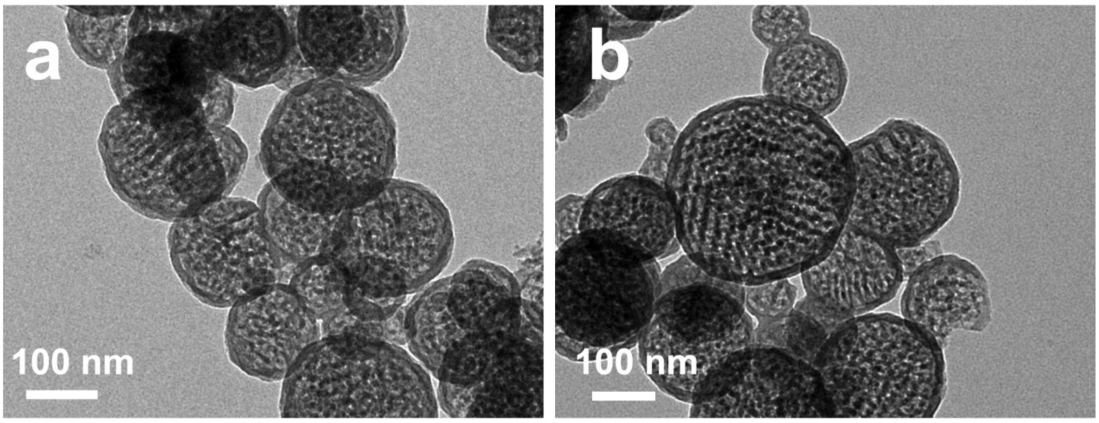

Fig. S12 TEM images of (a) HN-CSMCNs-12 and (b) HN-CSMCNs-15.

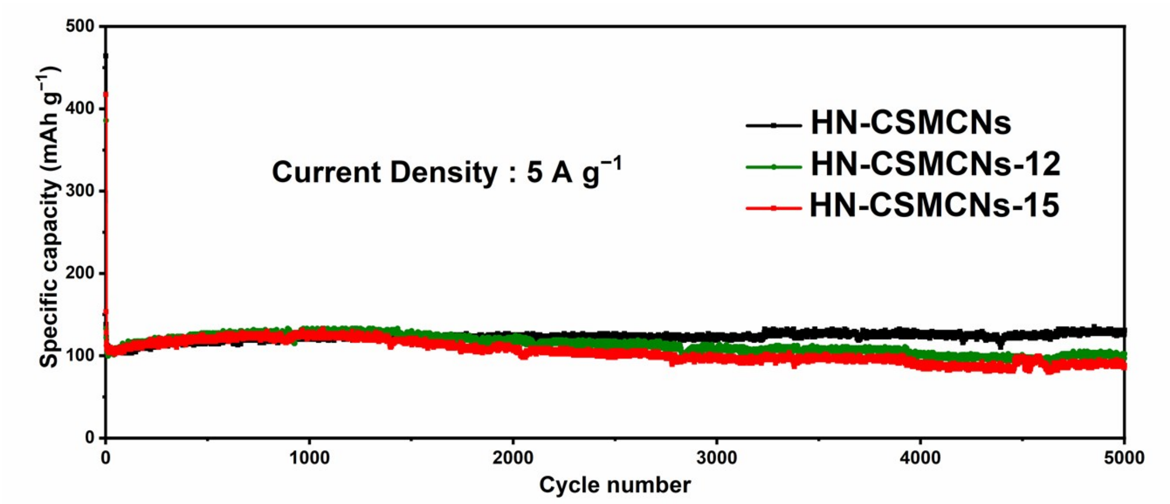

Fig. S13 Cycling performances of HN-CSMCNs, HN-CSMCNs-12 and HN-CSMCNs-15 at 5 A g^{-1}.

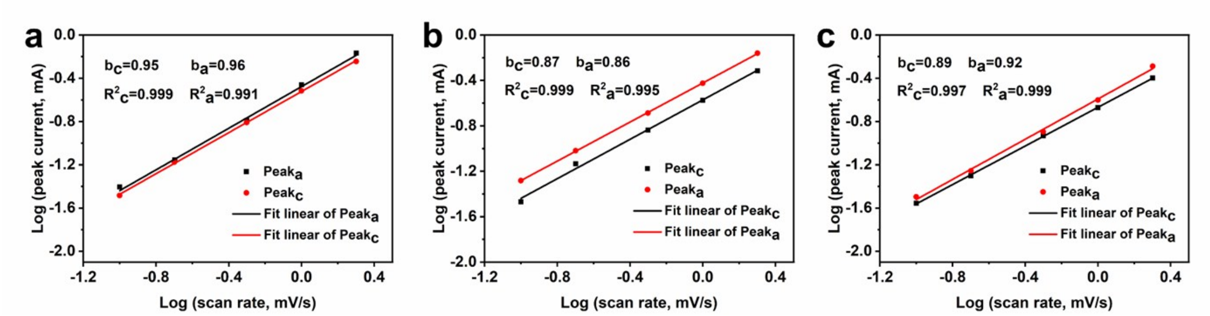

Fig. S14 Log(i) *vs.* log(v) plots of the cathodic and anodic peaks for (a) HN-CSMCNs, (b) HN-HCNs and (c) N-CSMCNs.

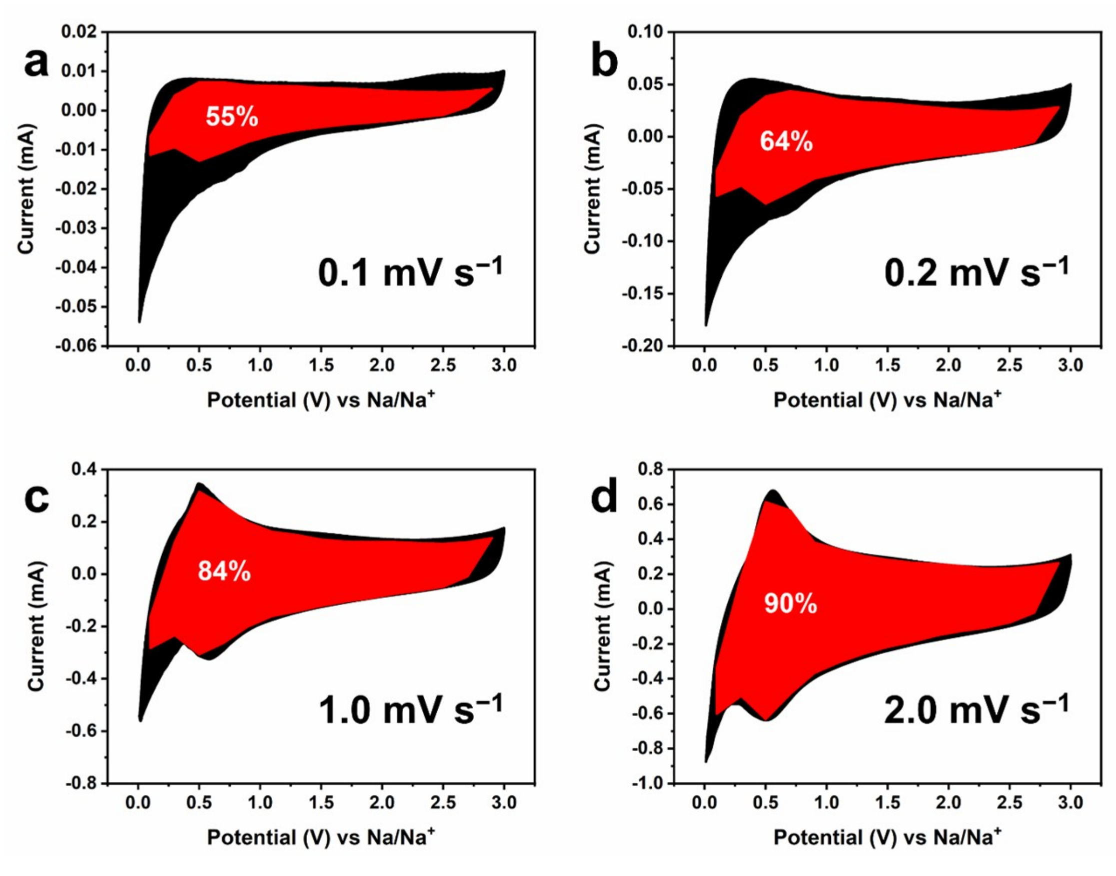

Fig. S15 Pseudocapacitive contributions (the red-filled area) of HN-CSMCNs at varied scan rates: (a) 0.1 mV s^{-1}, (b) 0.2 mV s^{-1}, (c) 1.0 mV s^{-1}, (d) 2.0 mV s^{-1}.

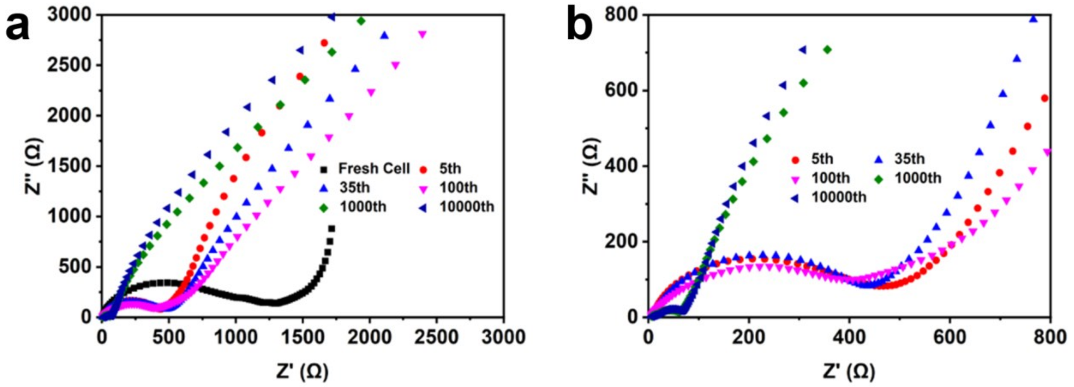

Fig. S16 Nyquist plots of HN-CSMCNs before and after cycling for different cycles in different magnification.

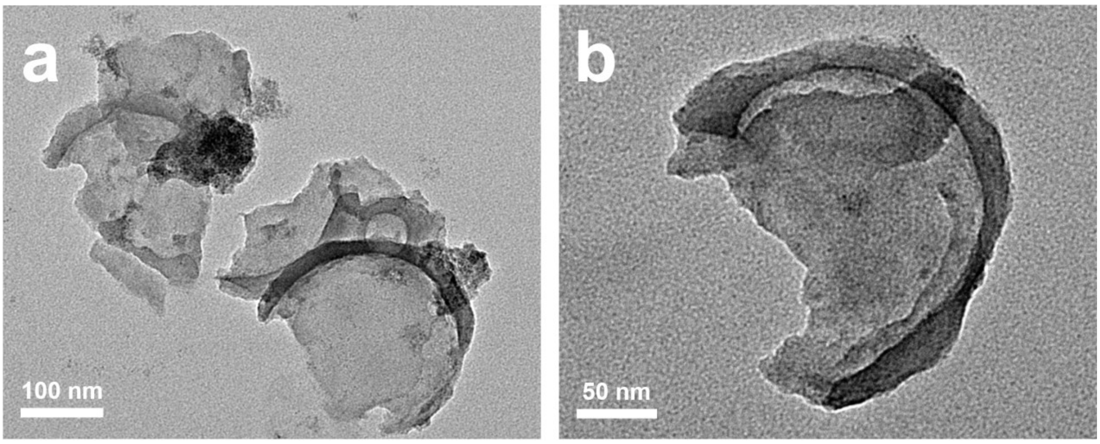

Fig. S17 TEM images of HN-HCNs after cycling for 10000 cycles at 5 A g^{-1}.

Table S3 Comparison of the performances of various carbonaceous materials for SIBs anodes reported recently.

Materials	Specific Capacity	High-rate Capability	Cycling performance	ICE	Ref.
HN-CSMCNs	251 mAh g^{-1} at 0.1 A g^{-1}	104 mAh g^{-1} at 15 A g^{-1}	■ **205 mAh/g after 1000 cycles at 0.5 A g^{-1}** ■ **163 mAh/g after 10000 cycles at 5 A g^{-1}** ■ **140 mAh/g after 20000 cycles at 10 A g^{-1}**	27.3%	**This work**
Hierarchically Porous, Active Carbon	248 mAh g^{-1} at 0.1 A g^{-1}	101 mAh g^{-1} at 5 A g^{-1}	169 mAh g^{-1} after 270 cycles at 0.5 A g^{-1}	18.5%	**[S1]**
Nanocarbon Network	280 mAh g^{-1} at 0.1 A g^{-1}	143 mAh g^{-1} at 0.5 A g^{-1}	296 mAh g^{-1} after 200 cycles at 0.05 A g^{-1}	48.2%	**[S2]**
N-doped Carbon Nanosheets	270 mAh g^{-1} at 0.1 A g^{-1}	139 mAh g^{-1} at 5 A g^{-1}	160 mAh g^{-1} after 9500 cycles at 1A g^{-1}	35.7%	**[S3]**
N-doped Hard Carbon Nanoshells	247 mAh g^{-1} at 0.1 A g^{-1}	63 mAh g^{-1} at 5 A g^{-1}	174 mAh g^{-1} after 200cycles at 0.1 A g^{-1}	30.4%	**[S4]**
N/S-doped Carbon Films	400 mAh g^{-1} at 0.1 A g^{-1}	92 mAh g^{-1} at 2 A g^{-1}	397 mAh g^{-1} after 1000 cycles at 0.1 A g^{-1}	63.5%	**[S5]**
N-rich Hierarchically Porous Carbon	250mAh g^{-1} at 0.1 A g^{-1}	150 mAh g^{-1} at 2 A g^{-1}	101.4 mAh g^{-1} after 10000 cycles at 5 A g^{-1}	51.2%	**[S6]**
3D Amorphous Carbon	240 mAh g^{-1} at 0.15 A g^{-1}	81 mAh g^{-1} at 4.8 A g^{-1}	188 mAh g^{-1} after 600 cycles at 0.3 A g^{-1}	75%	**[S7]**

References

[S1] X. Deng, W. Shi, Y. Zhong, W. Zhou, M. Liu, Z. Shao, *ACS Appl. Mater. Interfaces*, 2018, **10**, 21573−21581.

[S2] H. Jia, N. Sun, M. Dirican, Y. Li, C. Chen, P. Zhu, C. Yan, J. Zang, J. Guo, J. Tao, *ACS Appl. Mater. Interfaces*, 2018, **10**, 44368−44375.

[S3] J. Qin, H.M.K. Sari, C. He, X. Li, *J. Mater. Chem. A*, 2019, **7**, 3673−3681.

[S4] S. Huang, Z. Li, B. Wang, J. Zhang, Z. Peng, R. Qi, J. Wang, Y. Zhao, *Adv. Funct. Mater.*, 2018, **28**, 1706294.

[S5] J. Ruan, T. Yuan, Y. Pang, S. Luo, C. Peng, J. Yang, S. Zheng, *Carbon*, 2018, **126**, 9−16.

[S6] X. Hu, X. Sun, S.J. Yoo, B. Evanko, F. Fan, S. Cai, C. Zheng, W. Hu, G.D. Stucky, *Nano Energy*, 2019, **56**, 828−839.

[S7] P. Lu, Y. Sun, H. Xiang, X. Liang, Y. Yu, *Adv. Energy Mater.*, 2018, **8**, 1702434.